

# Integrating immunoinformatics and computational epitope prediction for a vaccine candidate against respiratory syncytial virus

Truc Ly Nguyen<sup>a</sup>, Heebal Kim<sup>a, b, c, \*</sup>

<sup>a</sup> Department of Agricultural Biotechnology and Research Institute of Agriculture and Life Sciences, Seoul National University, Seoul, 08826, Republic of Korea

<sup>b</sup> Interdisciplinary Program in Bioinformatics, Seoul National University, Seoul, 08826, Republic of Korea

<sup>c</sup> eGnome, Inc., Seoul, 05836, Republic of Korea

## ARTICLE INFO

### Article history:

Received 12 February 2024

Received in revised form 4 April 2024

Accepted 10 April 2024

Handling Editor: Dr Yijun Lou

### Keywords:

Respiratory syncytial virus

Multiepitope vaccine

Immunoinformatics

Docking molecular

Molecular dynamics simulation

Immune simulation

## ABSTRACT

Respiratory syncytial virus (RSV) poses a significant global health threat, especially affecting infants and the elderly. Addressing this, the present study proposes an innovative approach to vaccine design, utilizing immunoinformatics and computational strategies. We analyzed RSV's structural proteins across both subtypes A and B, identifying potential helper T lymphocyte, cytotoxic T lymphocyte, and linear B lymphocyte epitopes. Criteria such as antigenicity, allergenicity, toxicity, and cytokine-inducing potential were rigorously examined. Additionally, we evaluated the conservancy of these epitopes and their population coverage across various RSV strains. The comprehensive analysis identified six major histocompatibility complex class I (MHC-I) binding, five MHC-II binding, and three B-cell epitopes. These were integrated with suitable linkers and adjuvants to form the vaccine. Further, molecular docking and molecular dynamics simulations demonstrated stable interactions between the vaccine candidate and human Toll-like receptors (TLR4 and TLR5), with a notable preference for TLR4. Immune simulation analysis underscored the vaccine's potential to elicit a strong immune response. This study presents a promising RSV vaccine candidate and offers theoretical support, marking a significant advancement in vaccine development efforts. However, the promising *in silico* findings need to be further validated through additional *in vivo* studies.

© 2024 The Authors. Publishing services by Elsevier B.V. on behalf of KeAi Communications Co. Ltd. This is an open access article under the CC BY-NC-ND license (<http://creativecommons.org/licenses/by-nc-nd/4.0/>).

## 1. Introduction

RSV is a significant viral pathogen, particularly affecting the respiratory system, and is a leading cause of upper and lower respiratory tract infections, especially in infants and young children globally (Broor et al., 2018). Furthermore, RSV infects individuals with weakened immune systems or chronic lung/heart diseases and the elderly, where it can exacerbate the underlying diseases and account for the development of asthma, chronic obstructive pulmonary disease, and congestive heart

\* Corresponding author. Department of Agricultural Biotechnology, Seoul National University, Seoul 08826, Republic of Korea.

E-mail address: [heebal@snu.ac.kr](mailto:heebal@snu.ac.kr) (H. Kim).

Peer review under responsibility of KeAi Communications Co., Ltd.

failure (Falsey et al., 2005; Nam et al., 2019). First identified in 1956, RSV has since garnered attention due to its widespread prevalence, causing seasonal outbreaks and contributing to substantial morbidity and mortality worldwide (Borchers et al., 2013; Morris et al., 1956). RSV is ubiquitous and triggers outbreaks of respiratory infections, which tend to peak during the winter in temperate regions and the rainy season in tropical areas (Nam et al., 2019; Obando et al., 2018). The virus spreads through respiratory droplets, making it highly contagious (Bergeron et al., 2021). Virtually all children will have been infected with RSV by the age of two, and re-infections are common throughout life (Ruckwardt et al., 2019). In infants, RSV infections can cause crepitation, chest wall indrawing, hypoxemia, wheezing, and tachypnea, whereas, in adults, it can aggravate the underlying cardiopulmonary diseases (Broor et al., 2018; Ruckwardt et al., 2019). Premature birth, congenital heart disease, neuromuscular diseases, bronchopulmonary dysplasia, and male gender are the major risk factors of RSV infection (Messina et al., 2022). Among infants, RSV stands as the primary cause of hospitalizations worldwide and the second most prevalent cause of mortality in low- and middle-income nations. On a global scale, it has been approximated that RSV gives rise to 33 million new cases of acute lower respiratory tract infection in children under the age of five, leading to around 3 million hospitalizations and 120,000 deaths each year (Colosia et al., 2023; Mejias et al., 2019). In adults who contract RSV infection, mild cold-like symptoms are typical, and a few cases may progress to pneumonia or lung infection. Annually, approximately 60,000 to 160,000 older adults in the United States are hospitalized due to RSV infection, resulting in 6000 to 10,000 deaths (Harris, 2023).

While RSV infections are often mild and self-limiting, severe cases can lead to significant morbidity and mortality, particularly in infants and older adults. Due to the health risks and mortality linked to RSV, there has been a persistent demand for effective therapeutics for either treating or preventing RSV infections and associated illnesses (Colosia et al., 2023). The SARS-CoV-2 pandemic has heightened the awareness within the scientific community to prepare for highly contagious human viruses proactively. Therefore, it is imperative to explore innovative strategies for developing potential therapies against RSV, aiming to avert potential calamities in the future. Hence, in this study, the immunoinformatics and computational approaches have been integrated to develop a potential vaccine candidate against RSV. Firstly, the structural proteins from both subtypes of RSV were employed to identify antigenic B-cell and T-cell epitopes. Subsequently, the epitopes' properties were predicted, including allergic potential, antigenic potential, toxic property, and their capacity to elicit interferon-gamma (IFN- $\gamma$ ) and interleukin-4 (IL4). Then, the conservancy of these epitopes was determined in different RSV strains belonging to subtype A and subtype B of RSV, followed by the population coverage analysis of the T-cell epitopes. Afterward, chosen epitopes were linked with adjuvants and linkers to formulate an RSV vaccine candidate, for which we predicted physicochemical properties, stability, antigenicity, toxicity, and allergenicity. Following this, the vaccine candidate's tertiary structure was expected, then molecular docking and molecular dynamics simulation studies were conducted to elucidate its interactions with immune cells. Finally, an immune simulation study was carried out to assess how the designed RSV vaccine triggers immune responses in humans at various dosages. This research contributes to the ongoing efforts to address the challenges posed by RSV and underscores the potential of immunoinformatics in advancing vaccine design against respiratory pathogens.

## 2. Materials and methods

### 2.1. Protein sequence retrieval and epitope prediction

Protein sequences of RSV structural proteins were retrieved from UniProt database (Consortium, 2022). T-helper cell epitopes, capable of binding to MHC class II molecules, were predicted using the NetMHCII 2.3 server (Jensen et al., 2018). Similarly, T-cytotoxic cell epitopes with potential for MHC class I molecule binding were predicted using the NetMHCpan 4.0 web server (Andreatta et al., 2016). Protein sequences were input in FASTA format into the NetMHCpan 4.0 and NetMHCII 2.3 servers, with chosen peptide lengths of 9 and 15 (default) respectively. Default parameters of the NetMHCpan 4.0 and NetMHCII 2.3 servers were applied to establish thresholds for strong and weak binders. For predicting multiple linear B-cell epitopes, the BepiPred 2.0 server was employed (Larsen et al., 2006). Subsequently, the antigenicity of predicted B-cell and T-cell epitopes was determined using the VaxiJen v2.0 web server (Doytchinova et al., 2007). The epitope's allergic potential, toxicity, and IFN- $\gamma$  activation potential were assessed using the AllergenFP v1.0, ToxinPred, and IFNepitope web servers, respectively (Dhanda et al., 2013; Dimitrov et al., 2013; Gupta et al., 2013). Additionally, the IL4pred server was employed to evaluate the epitopes' capability to induce interleukin-4 (IL4) production (Dhanda et al., 2013b).

### 2.2. Conservancy analysis and population coverage analysis

The study aims to develop a vaccine candidate against both the subtypes of RSV. Hence, the conservancy of the predicted epitopes that were antigenic, non-toxic, non-allergic, and induced cytokine generation was performed by employing the Immune Epitope Database and Analysis Resources (IEDB) tool (Bui et al., 2007). Within this tool, epitope and protein sequences from various RSV strains of both subtypes were inputted in FASTA format, and opting for the default settings for all other parameters. The IEDB population coverage analysis tool was utilized to ascertain population coverage for the selected T-cell epitopes in the design of the vaccine candidate (Bui et al., 2006). Notably, determining population coverage analysis for the final B-cell epitopes proved challenging due to the absence of web servers or software capable of predicting B-cell epitope population coverage. The IEDB population coverage analysis tool employed default values for the "number of epitopes" and

"query by" parameters. The selection "World" was made for "select area(s) and population(s)," and the combined Class I and II options were chosen under the "select calculation option."

### 2.3. Vaccine candidate engineering and physicochemical properties prediction

The selected B-cell and T-cell epitopes were conjugated with flagellin, RS09 adjuvants, and the PADRE (Pan HLA DR-binding epitope) sequence through the use of GGS linkers, forming the final vaccine construct. The GGS linker, chosen for its flexibility and biocompatibility, facilitated the integration of adjuvants and epitopes, enhancing the vaccine's immunogenic potential. The ExPasy ProtParam tool was used to evaluate the vaccine construct's physicochemical properties, such as molecular weight, isoelectric point, aliphatic index, and stability. Antigenicity was predicted using the Vaxijen v2.0 tool, assessing the vaccine's potential to elicit an immune response (Doytchinova et al., 2007; Gasteiger et al., 2005).

### 2.4. Prediction, refinement, and validation of the tertiary structure of the vaccine candidate

The tertiary structure of the vaccine candidate was predicted using AlphaFold2's deep learning algorithm through ColabFold v1.5.5 (Jumper et al., 2021), with subsequent structural refinement performed on the GalaxyWEB server (Ko et al., 2012). Model quality and validation were thoroughly assessed using ProSA-web (Wiederstein et al., 2007), PROCHECK program (Laskowski et al., 1993), and QMEAN4 (Benkert et al., 2010; Chawla et al., 2023), ensuring a comprehensive evaluation of the vaccine candidate's structure.

### 2.5. Molecular docking studies between the vaccine and immune receptors

The structure of the human TLR4 (UniProt ID: O00206) and TLR5 receptor (UniProt ID: O60602) were predicted by AlphaFold2. For both receptors, we retained only the extracellular domain encompassing amino acids 30–624 of TLR4 and 21–639 of TLR5, while excluding other regions. The 3D structure of the multi-epitope vaccine (MEV) candidate and immune receptors were docked using the ClusPro server (Kozakov et al., 2017). ClusPro conducts molecular docking analysis through a multi-step process that includes rigid body docking, clustering of low-energy structures, and energy minimization. Initially, it employs rigid body docking, where billions of conformations are sampled. Subsequently, the 1000 lowest energy structures are grouped to identify the largest clusters, based on root-mean-square deviation (RMSD). Finally, energy minimization is conducted to eliminate steric clashes, refining the docking results (Nguyen et al., 2024a). Accordingly, the complex displaying the lowest binding energy (in kcal/mol) was selected for visualization. PDBsum was subsequently employed to analyze and identify interacting residues between the vaccine and TLR4/TLR5 receptors (Laskowski et al., 2018).

### 2.6. Molecular dynamics simulations of the vaccine-receptor complex

To investigate the stability of the vaccine-receptor complex, all-atom molecular dynamics (MD) simulations were performed using the GROMACS 2023 software on a Linux operating system employing the CHARMM27 force field (Abraham et al., 2015). The docking complex MEV-TLR4 was solvated in a cubic box ( $12 \times 12 \times 12$ ) using the SPCE water model, surrounded by 325,909 solvent molecules. Subsequently, to neutralize the charge, 24  $\text{Na}^+$  ions were added. The system underwent energy minimization, using the steepest descent algorithm with 50,000 steps, and the minimization process ceased when the maximum force reached  $<1000.0$  kJ/mol/nm. Following that, position restraints were applied during the equilibration process. NVT equilibration was executed at 300 K with 50,000 steps (100 ps), followed by NPT equilibration at 1 bar reference pressure with an additional 50,000 steps (100 ps). Afterward, a production simulation for all-atom (995,112 atoms) was conducted using the NPT ensemble for 50,000,000 steps (100 ns). Upon completing the 100 ns MD simulation, we computed the root mean square deviation (RMSD) of backbone residues, root mean square fluctuation (RMSF) of C-alpha, the solvent-accessible surface area (SASA), and the buried surface area (BSA) for the system. To validate result accuracy and reliability, three replicate MD simulations were performed over 100 ns with a different starting velocity (Akhtar et al., 2022; Kaushik et al., 2022a). Additionally, superimpositions of the docking complex were created using selected snapshots from the MD simulations. Finally, the COCOMAPS tool (Vangone et al., 2011) was employed to examine interface connectivity between the MEV and TLR4 through specific snapshots.

### 2.7. Computational immune simulation of RSV vaccine candidate

An *in silico* immune simulation was performed using the C-IMMSIM online tool, applying default settings with the exception of the time step adjustment, to explore the immune response elicited by the RSV vaccine construct (Rapin et al., 2011). Although the recommended interval between two vaccine doses is typically four weeks, intervals ranging from 8 weeks to 6 months can also be considered, depending on the instance (Castiglione et al., 2012; Robinson et al., 2017). Accordingly, to assess the immune response to the RSV vaccine construct, three doses were administered at four-week intervals. The time steps used in the simulation were 1, 84 (representing 4 weeks), and 168 (corresponding to 8 weeks).

### 3. Results

#### 3.1. Protein sequence retrieval and epitope prediction

The UniProt IDs of the structural proteins of RSV strain A2 belonging to subtype A have been provided in Table 1. All retrieved proteins were verified at the protein level, each receiving a top annotation score of 5/5, with the exception of the M2-2 protein. A total of 749 strong-binding MHC-I epitopes, 1621 high-affinity MHC-II epitopes, and 36 linear B-cell epitopes were predicted from the RSV structural proteins (Supplementary Data Sheets). Then, these epitopes underwent further analysis for antigenicity (Vaxijen score above 0.4), allergenicity, toxicity, and ability to induce IFN- $\gamma$  and IL-4. These comprehensive analyses led to the identification of 22 MHC-I epitopes and 72 MHC-II epitopes, with only 6 B-cell epitopes meeting the specified criteria.

#### 3.2. Conservancy analysis and population coverage analysis

Epitope conservancy was assessed across the S2 strain (A subtype), 9320 strain (B subtype), and B1 strain (B subtype) RSV strains. Sequences of all the structural proteins are available in UniProt for only these RSV strains, whereas other strains have only 1 or 2 protein sequences documented. Among the 22 MHC-I epitopes, 14 showed conservancy in all the selected strains. Likewise, 31 of the 72 MHC-II epitopes were conserved across these RSV strains. Three of the 6 B-cell epitopes were conserved in the tested RSV strains. To narrow down the epitope selection for the vaccine construct, a further parameter - a Vaxijen score above 1.1 - was applied. Consequently, 6 MHC-I and 5 MHC-II binding epitopes were selected for the final construct, achieving a global population coverage of 52.07%, as detailed in Table S1.

#### 3.3. Vaccine candidate engineering and physicochemical properties prediction

Following comprehensive analysis in the earlier sections, 6 MHC-I binding epitopes, 5 MHC-II binding epitopes, and 3 B-cell epitopes were shortlisted for the vaccine design (Table 2). Each selected epitope is antigenic, non-allergic, non-toxic, capable of inducing of IFN- $\gamma$  and IL-4, and conserved in all tested strains. These selected epitopes were then integrated with flagellin adjuvant, RS09 adjuvant, and PADRE sequence using appropriate linkers GGS, as outlined in the methodology, to form an RSV vaccine candidate composed of 545 amino acids (Table S2). Additionally, Table S3 presents the physicochemical parameters of the vaccine candidate, which is characterized by its antigenicity, non allergenicity, non toxicity, and stability.

**Table 1**  
UniProt IDs of the structural proteins of RSV strain A2.

Protein	UniProt ID	Identification method	Annotation score
N: Nucleoprotein	P03418	Evidence at protein level	5/5
P: Phosphoprotein	P03421	Evidence at protein level	5/5
M: Matrix protein	P0DOE7	Evidence at protein level	5/5
SH: Small hydrophobic protein	P0DOE5	Evidence at protein level	5/5
G: Major surface glycoprotein	P03423	Evidence at protein level	5/5
F: Fusion glycoprotein	P03420	Evidence at protein level	5/5
M2-1	P04545	Evidence at protein level	5/5
M2-2	P88812	Inferred from homology	2/5
L: RNA-directed RNA polymerase	P28887	Evidence at protein level	5/5

**Table 2**  
Epitopes for the design of the final RSV vaccine candidate.

Protein	MHC type	Epitopes	Binding MHC alleles	Vaxijen score <sup>a</sup>
Nucleoprotein	MHC-I	EMKFEVLTL	HLA-B*08:01	1.1076
Matrix protein		EKDDDPASL	HLA-B*39:01	1.343
Fusion glycoprotein		ASISQVNEK	HLA-A*03:01	1.3852
RNA-directed RNA polymerase		DIRYIYRSL	HLA-B*08:01	1.3203
		ELEYRGESL	HLA-B*08:01	1.6945
		YHAQDDIDF	HLA-B*39:01	1.3715
Nucleoprotein	MHC-II	VFVHFGIAQSSTRGG	DRB1_0901	1.1723
Fusion glycoprotein		TDRGWYCDNAGSVSF	DRB3_0101	1.1909
RNA-directed RNA polymerase		TVVELHPDIRYIYRS	DRB1_0301	1.1211
		PWVVNIDYHPTHMKA	DRB1_0301	1.2262
		CPWVVNIDYHPTHMK	DRB1_0301	1.4633
Phosphoprotein	B-cell	ETFDNNEESSYSYEEINDQTNDNI	Not applicable	0.5306
RNA-directed RNA polymerase		ISNKSNNRYNDNYN	Not applicable	0.8783
		SRPCEFPASIPAYRT	Not applicable	0.4767

<sup>a</sup>Vaxijen score above 1.1 for MHC epitopes and 0.4 for B-cell epitopes.

### 3.4. Prediction, refinement, and validation of the tertiary structure of the vaccine candidate

The multi-epitope vaccine (MEV) construct was predicted using the cutting-edge AlphaFold2 via ColabFold v1.5.5. Given that, the AlphaFold2 prediction yielded a low score for specific residues (Fig. S1), and the calculated scores for Ramachandran plots yielded 60.4% residues in core acceptable region, 35.6% in allowed and generously allowed regions and 4.0% residues in disallowed regions (Fig. S2). To enhance the model's quality, we pursued further structural refinement using the GalaxyWEB server. Among models 1–5, model 1 (Fig. 1A) was determined to be the most accurately refined. The results in terms of improvement of model 1 over initial input models for backbone structure accuracy measured by GDT-HA, side-chain structure accuracy measured by RMSD, and physical correctness measured by MolProbity score were summarized in Table S4. Furthermore, to validate the model's quality, we calculated Z-Score with a value of  $-6.8$  (Fig. 1B), analyzed the Ramachandran plot (Fig. 1C), and determined QMEAN4 value of  $-4.27$  (Fig. 1D). According to the Ramachandran plot, 94.5% of residues were situated in the favorable core region, 5.1% in the allowed and generously allowed regions, and only 0.4% in the disallowed region. Hence, the refined MEV model (Fig. 1A) demonstrates a high quality, making it suitable for further studies.

### 3.5. Molecular docking of the vaccine candidate with immune TLR4 and TLR5 receptors

The tertiary structure of human TLR4 (UniProt ID: O00206) and TLR5 receptor (UniProt ID: O60602) were determined using AlphaFold2. The yield of high pLDDT values with confidence scores exceeding 90 for most residues indicated a high prediction confidence level for TLR4 (Fig. S3) and TLR5 (Fig. S4). The molecular docking was performed for two complex systems, MEV-TLR4 and MEV-TLR5, using the ClusPro server, which generated the top 30 models for each system. From these models, the ones with the lowest negative docking score were selected as the best-docked complexes. Specifically, the models with  $-1257.4$  kcal/mol (MEV-TLR4) and  $-1542.7$  kcal/mol (MEV-TLR5) were chosen for further analysis. Interactions between MEV and TLR4/TLR5 were illustrated in Fig. 2, visualized using the PDBsum database with default threshold values of 3.5 Å. Analysis revealed the formation of 60 hydrogen bonds and 8 salt bridges between MEV and TLR4 (Fig. 2A and Table S5), while MEV and TLR5 demonstrated only 19 hydrogen bonds (Fig. 2B and Table S6). These findings indicate MEV's strong binding affinity to TLR4, suggesting its potential to elicit an immune response.

### 3.6. Molecular dynamics simulation studies

Following the molecular docking outcomes, the MEV-TLR4 complex, identified as the optimal docking configuration, was selected for MD simulation studies. Three replicate of MD simulations 100 ns were conducted for all-atom to investigate the

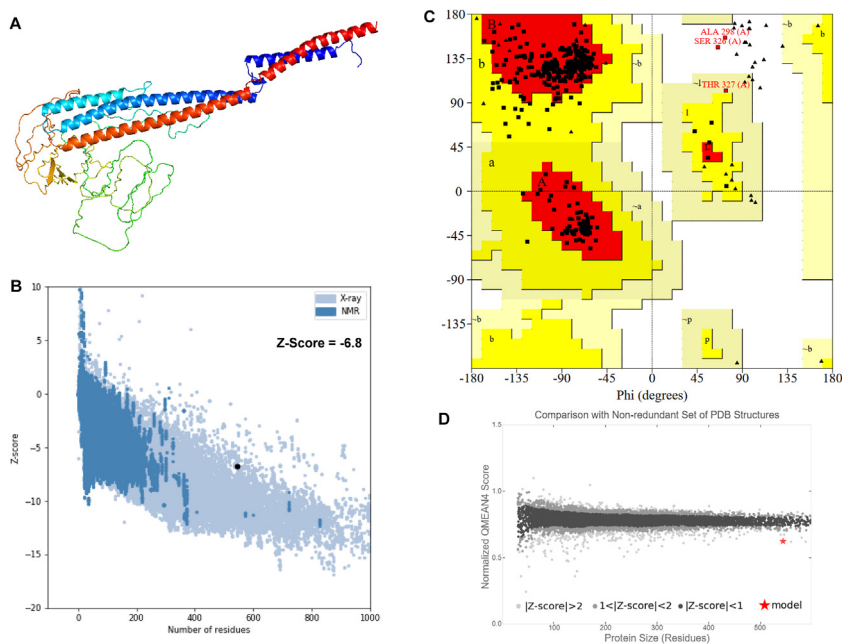


**Fig. 1.** Tertiary structure of the vaccine construct. (A) Refined model representation in a cartoon by the GalaxyWEB server. (B) Z-Score was obtained from the ProSA-web of the refined model. (C) Ramachandran plot using PROCHECK program. (D) Normalized QMEAN score composed of four statistical potential terms (QMEAN4) of the vaccine construct.

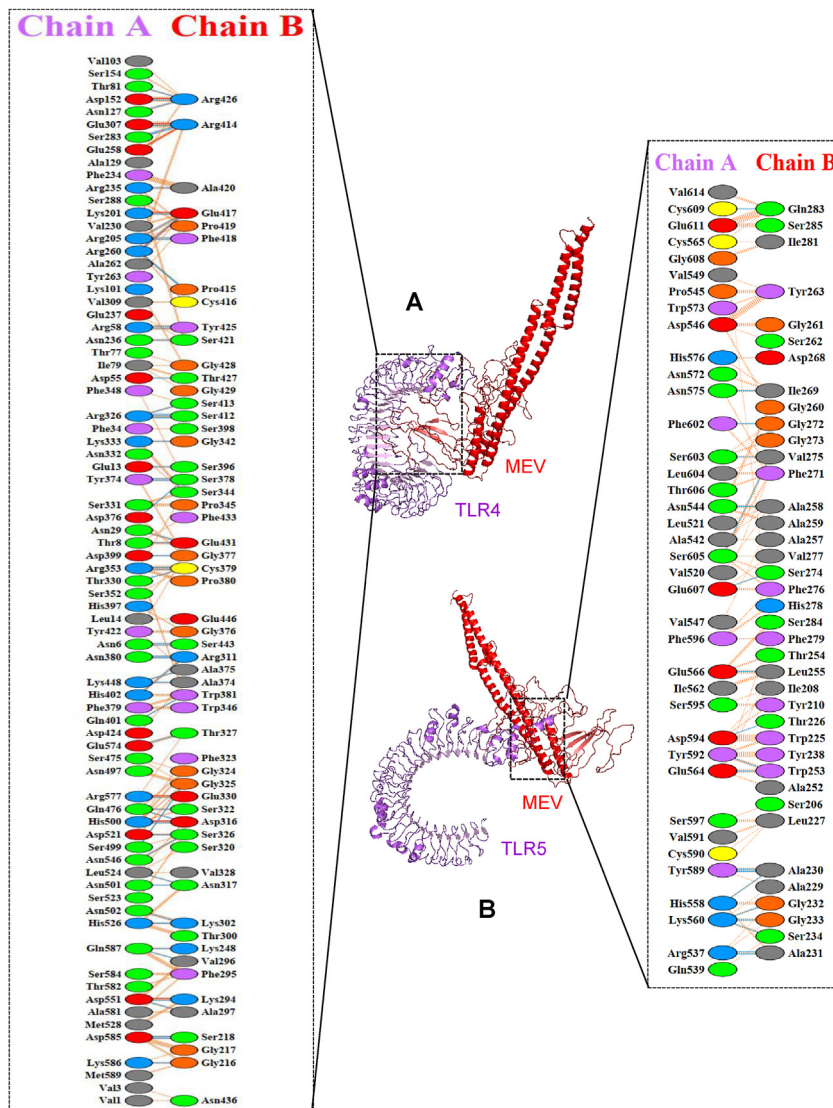


**Fig. 2.** Molecular docking between the MEV (red) and TLR4/TLR5 (purple). (A) Docking complex representation in cartoon and residue interactions between TLR4 (chain A) and MEV (chain B). (B) Docking complex representation in cartoon and residue interactions between TLR5 (chain A) and MEV (chain B). Salt bridges (red lines), hydrogen bonds (blue lines), and nonbonded contacts (orange dashed line) between residues on either side of the vaccine-receptor interface.

stability of the vaccine-receptor complex using GROMACS 2023 software on a Linux operating system, which provides real-life environmental conditions for various biological models (Nguyen et al., 2024b). RMSD from the backbone of the complex showed an average value of  $0.84 \pm 0.16$  nm, achieving stability after 20 ns simulation time (Fig. 3A). Besides, the RMSF was quantified to evaluate the flexibility across the amino acid residues within the complex. Fig. 3B shows RMSF values of  $0.53 \pm 0.32$  nm for the vaccine (residues 1 to 545) and  $0.34 \pm 0.08$  nm for TLR4 (residues 546 to 1140), indicating the vaccine exhibits greater flexibility than TLR4. Significant fluctuations were observed particularly in the N- and C-terminal regions of flagellin within the vaccine. Another measure of docking complex MEV-TLR4 behavior is the solvent-accessible surface area (SASA). The SASA is governed by the interactions (or lack of) of hydrophobic and hydrophilic amino acids with water. Fig. 3C presents an average SASA value of  $591.27 \pm 16.35$  nm<sup>2</sup>, with the complex achieving a steady state after 40 ns and maintained it throughout the simulation. Moreover, the buried surface area (BSA) at the MEV-TLR4 interface remained stable throughout the simulation, suggesting consistent interface interactions with a value of  $45.61 \pm 9.99$  nm<sup>2</sup> (Fig. 3D).

To further assess the complex's stability throughout the simulation, we calculated the RMSD of the MEV-TLR4 complex at various time steps. By comparing the stability of the MEV-TLR4 complex, we were able to determine their respective stability (Fig. 4A). Subsequently, the COCOMAPS tool was employed to thoroughly study and visualize the contact points at the MEV-TLR4 interface (Fig. 4B). Using intermolecular contact maps to find hot spot residues, COCOMAPS makes it possible to analyze

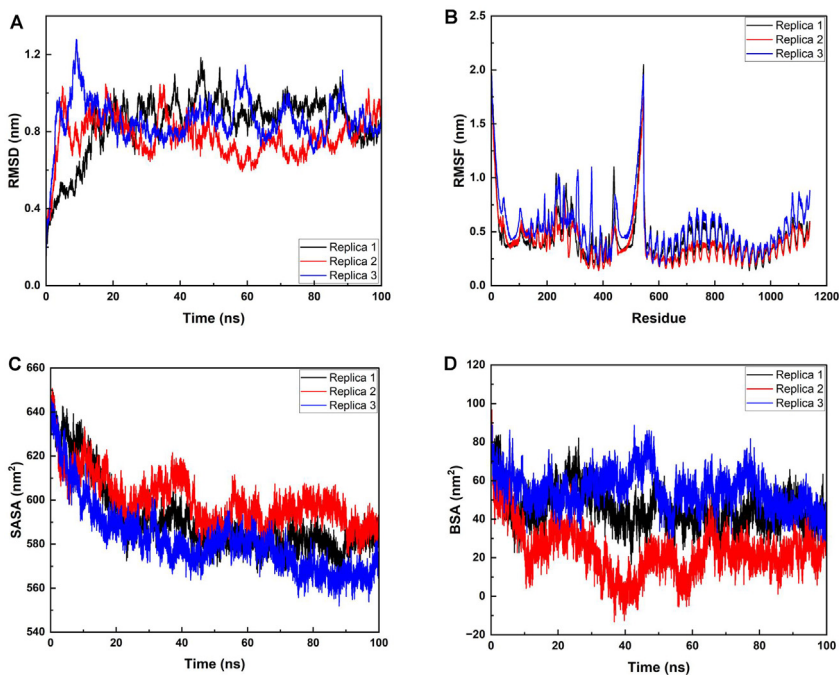


**Fig. 3.** Molecular dynamics simulation of the vaccine and TLR4 complex. (A) Root mean square deviation (RMSD). (B) Root mean square fluctuation (RMSF). (C) Solvent-accessible surface area (SASA). (D) Buried surface area (BSA).

and visualize the interaction interface in protein complexes (Vangone et al., 2011). While the study is presented for the chosen snapshots (Fig. 4A), where the interaction pattern with the contacts is maintained, it is clear from Fig. 4B that overall contacts remained steady (Akhtar et al., 2023; Kaushik et al., 2022b).

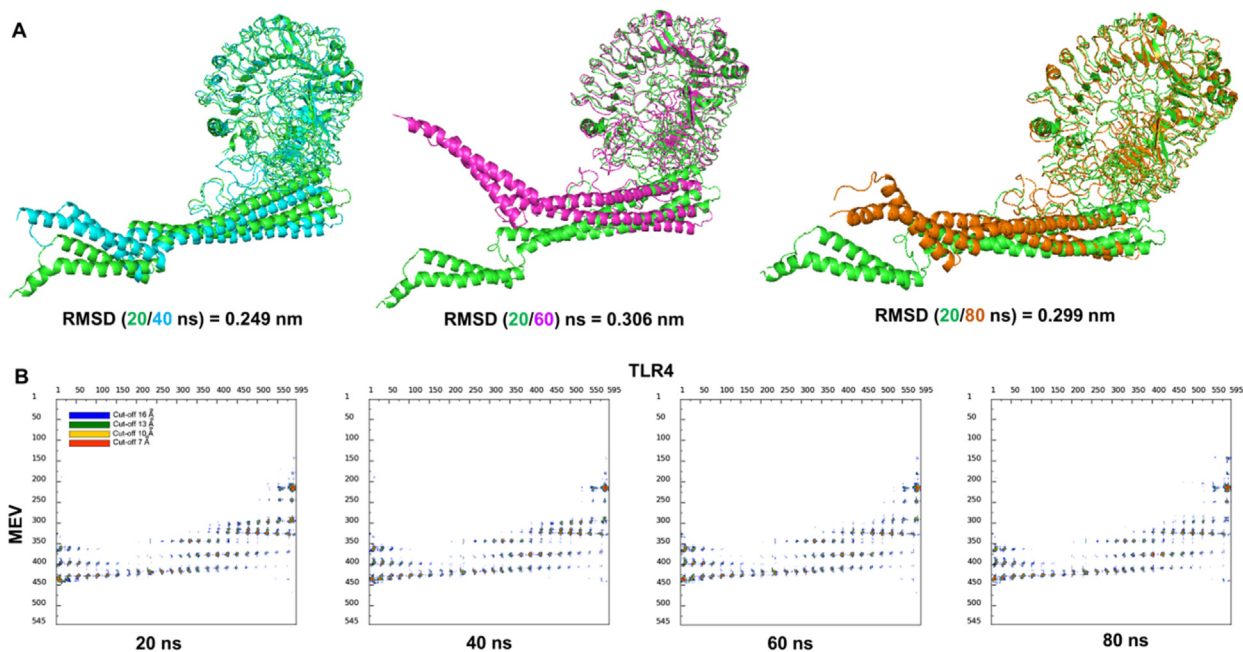


**Fig. 4.** Stability of the docking complex MEV-TLR4. (A) Superimposition of selected snapshots of MEV-TLR4 and their respective RMSD values. (B) Contact maps showing the conservation of contacts between residues in MEV and TLR4.

Remarkably, the interface area and percentage of polar to non-polar residues at the interface of modeled complexes were found to be nearly the same across all instances (Table 3). Besides, across all model complexes, employing a cut-off distance of 5 Å to define two residues in contact, the distribution of hydrophilic-hydrophobic, hydrophilic-hydrophilic, hydrophobic-hydrophobic, and hydrogen bonds exhibited minimal variation in the four selected structures (Table 3). All the above analyses demonstrate that the interaction patterns between TLR4 and MEV maintained stability throughout the simulation period.

### 3.7. Computational immune simulation of RSV vaccine candidate

A computational immune simulation was conducted to assess the immune responses elicited by the designed RSV vaccine. Fig. 5 displays the immune response patterns predicted from the computational analysis of the vaccine. Analysis of the initial dose (Fig. 5A) compared to subsequent doses reveals a significant increase in antibody concentrations, encompassing IgM + IgG, IgM, IgG1 + IgG2, and IgG1. This signifies that immunization with the candidate vaccine instigates an enhanced antibody response. Additionally, successive vaccine doses result in an increase in the total B-cell population, B-memory cell populations, and B isotype IgM population, underscoring the stimulation of a robust secondary immune response (Fig. 5B). Following each vaccination, there is an increase in the plasma B lymphocyte population as well (Fig. 5C). Furthermore, the active TH cell population increases after each immunization (Fig. 5D). However, the duplicating and resting TH cell population increases up to the second dose of the vaccine but decreases after the third dose of vaccination (Fig. 5D). Moreover, the vaccine candidate stimulates the production of various cytokines, including IFN- $\gamma$ , interleukin-10 (IL10), interleukin-12 (IL12), and transforming growth factor-beta (TGF- $\beta$ ) (Fig. 5E). Compared to the initial dose, the second dose of the vaccine results in an increased population of IFN-gamma, IL-10, TGF- $\beta$ , and IL-12. Following the third dose of the vaccine construct, there is an overall decrease in the concentration of different cytokines and interleukins compared to the first and second doses (Fig. 5E).

## 4. Discussion

RSV is an enveloped RNA virus belonging to the Paramyxoviridae family. There are two antigenically distinct RSV subtypes: A and B. These subtypes co-circulate within the same season, with one prevailing over the other. While specific studies indicate that subtype A is linked to heightened disease severity, others suggest that subtype B may have higher severity or that both subtypes exhibit comparable severity (Ciarlito et al., 2019; Laham et al., 2017; Shen et al., 2022; Vandini et al., 2017). RSV possesses a single-stranded, negative-sense RNA genome, encoding for 11 proteins of which three are non-structural (NS1, NS2, M2–2), and 8 are structural proteins namely major surface glycoprotein (G), fusion glycoprotein (F), small hydrophobic protein (SH), nucleoprotein (N), phosphoprotein (P), matrix protein (M), M2-1 and RNA-directed RNA polymerase (L) (Kiss et al., 2014). Two major surface glycoproteins, the F and G proteins, play crucial roles in viral entry and fusion with host cells. The F protein is particularly interested in vaccine development due to its role in entry into host cells, high conservation in RSV A and B subtypes, and the induction of protective immune responses. The G protein also bears antigenic determinants that trigger the production of neutralizing antibodies (Mejias et al., 2019). The L, N, M2-1, and P proteins envelop the viral RNA, creating a helical assembly known as the ribonucleoprotein complex, which protects the RNA (Cosentino et al., 2022; Kiss et al., 2014). The M2-1 protein helps regulate RSV organization and transcription process (Cosentino et al., 2022; Kiss et al., 2014). The M protein envelops the inner surface of the viral membrane, forming a protective layer around the viral genomic material (Conley et al., 2022). The deletion of the SH protein has slowed apoptosis in the infected cells and caused attenuation of the virus, suggesting the role of the protein in the pathogenesis of RSV (Li et al., 2015). Given these structural proteins' role in RSV's infection and pathogenesis, our study targeted them to identify epitopes for the potential vaccine design against RSV.

The US Food and Drug Administration (FDA) approved using the antiviral ribavirin in the aerosolized form for treating RSV infection in 1998. However, ribavirin offers limited clinical advantages in RSV and is not commonly prescribed as a routine treatment (Colosia et al., 2023; Mir et al., 2021). Similarly, the FDA approved the monoclonal antibody palivizumab to prevent RSV-associated severe lower respiratory tract infections in pediatric patients in 1996 (Garegnani et al., 2021). Presently, extensive research, encompassing clinical trials, is underway to develop treatments or preventive measures for RSV. One of the extensively researched areas for developing therapies against RSV is the area of vaccine development. Different vaccine candidates, such as subunit-based, live attenuated, nucleic acid, and vector-based, have been explored to protect infants, children, and elderly patients (Bergeron et al., 2021; Ruckwardt, 2023; Topalidou et al., 2023). Currently, the FDA has licensed

**Table 3**  
The stability of interface interactions between MEV and TLR4.

Modeled complex	Interface area Å <sup>2</sup>	Polar residue (%)	Non-polar residue (%)	Hydrophilic-Hydrophobic contacts	Hydrophilic-Hydrophilic contacts	Hydrophobic-Hydrophobic contacts	H-bonds
20 ns	2767.55	58.48	41.52	129	105	28	32
40 ns	2572.0	59.14	40.86	128	98	30	29
60 ns	2604.95	57.54	42.46	140	99	26	30
80 ns	2407.7	57.35	42.65	128	86	22	29

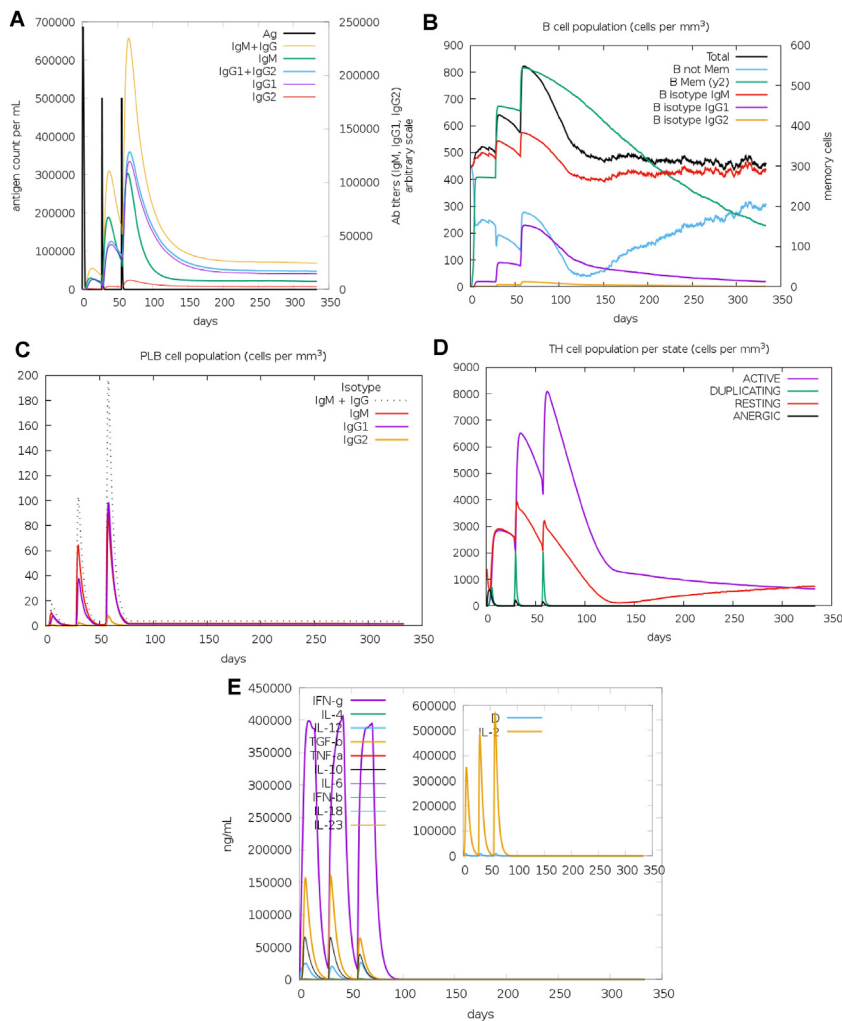


**Fig. 5.** Immune simulation of the RSV vaccine construct. (A) Antigen and immunoglobulins. Antibodies are sub-divided per isotype. (B) B lymphocytes: total count, memory cells, and sub-divided in isotypes IgM, IgG1 and IgG2. (C) Plasma B lymphocytes count sub-divided per isotype (IgM, IgG1 and IgG2). (D) CD4 T-helper lymphocytes count sub-divided per entity-state (i.e., active, resting, anergic, and duplicating). (E) Concentration of cytokines and interleukins. D in the inset plot is danger signal.

two vaccines, Abrysvo and Arexvy, developed by Pfizer and GSK, respectively, and the 24 other candidates are under clinical trial stages (Topalidou et al., 2023). Furthermore, different groups have also explored the immunoinformatics approach to design a vaccine candidate against RSV (Dar et al., 2022; Moin et al., 2023; Naqvi et al., 2021; Tahir Ul et al., 2020). Nevertheless, our study's methodology, tools, and targeted proteins differ from those in previous research. Dar et al. focused on RSV's F and G proteins to predict antigenic epitopes (Dar et al., 2022). Moin et al. targeted the N, P, F, and G proteins to predict T-cell and B-cell epitopes for making vaccine candidates against both RSV subtypes. Still, the computational tools utilized in our study differ from those in Moin et al.'s paper (Moin et al., 2023). Similarly, Naqvi et al. targeted the F, G, and SH proteins to predict only T-cell epitopes for the RSV vaccine candidate design (Naqvi et al., 2021). Additionally, Tahir et al. targeted the RSV F and G proteins to design a vaccine candidate following a methodology different from ours (Tahir Ul et al., 2020).

This study's immunoinformatics analysis identified 6 MHC-I, 5 MHC-II, and 3 B-cell epitopes within RSV's structural proteins. These selected epitopes were found to be antigenic, non-toxic, conserved among both the subtypes of RSV, non-allergic, and elicited the generation of IFN- $\gamma$  and IL-4. The induction of the IFN- $\gamma$  and IL-4 by the epitopes suggests the potential role of the epitopes in thwarting viral replication and activation of innate and adaptive immune activities (Cordeiro et al., 2022; Dittmer et al., 2001). The selected epitopes' conservancy suggests that our vaccine candidate could offer effective protection against both the RSV subtypes. Flagellin protein, RS09, and PADRE adjuvants were implemented to enhance the vaccine construct's efficacy. RS09 functions as an agonist of TLR4, while the flagellin protein acts as a TLR5 agonist (Forstneric et al., 2017; Gupta et al., 2014; Shanmugam et al., 2012). The TLR agonists play a crucial role in activating innate and adaptive immunity. Incorporating PADRE into the MEV can elevate its immunogenicity and efficacy (Ma et al., 2020).

PADRE exhibits a high-affinity binding ability to various MHC class II molecules, facilitating the generation of antigen-specific CD4<sup>+</sup> T-cell responses (Ghaffari-Nazari et al., 2015). Additionally, it has also been reported to elicit CD8<sup>+</sup> T-cell responses (Ma et al., 2020). This attribute has led to its widespread utilization in the construction of MEVs. Proteins under 110 kDa are considered suitable for vaccine candidates (Shen et al., 2022), and our RSV vaccine's molecular weight is 57.22 kDa, affirming its appropriateness. Furthermore, the designed vaccine exhibits no homology with human proteins, thereby minimizing the risk of autoimmune responses in the vaccine recipients. The final vaccine protein displays an instability index of 38.74, suggesting stability in biological conditions, as compounds with an instability index below 40 are considered stable.

Moreover, molecular docking and dynamics simulations were performed to understand the MEV's interactions with TLR4 and TLR5, confirming these interactions' stability. Significantly, our results showed stronger and more stable interactions between the MEV and TLR4 than with TLR5. This aligns with the outcomes of previous investigations (Marzec et al., 2019; Monick et al., 2003). In that study, Monick et al. demonstrated that TLR4 was more highly expressed and found in the membrane when lung epithelial cells (primary and transformed cell lines) were infected with RSV (Monick et al., 2003). Meanwhile, J. Marzec et al. suggested that TLR4 played a role in the pathogenesis of pulmonary RSV and the activation of cellular immunity caused by the inflammasome complex and vascular damage. Additionally, in line with computational immune simulation, the designed RSV vaccine construct is anticipated to have the potential to induce robust immune responses in recipients.

## 5. Conclusion

An advanced bioinformatics approach has been utilized in this study to design a promising vaccine against RSV. Through comprehensive computational analyses, we predicted antigenic, non-allergic, and non-toxic T-cell and B-cell epitopes. The vaccine's formulation, enriched with adjuvants and linkers, aims to boost its overall effectiveness. Population coverage analyses and detailed physiochemical evaluations further validated the potential of our vaccine candidate. Furthermore, molecular docking, MD simulations, and immune simulations underscored stable interactions with immune cells, enhancing confidence in its immunogenic potential. In summary, this research employed immunoinformatics and computational methods to design and evaluate a potential RSV vaccine, marking a significant stride in vaccine development efforts. The integration of these strategies has not only streamlined the vaccine development process but also opened new pathways for combating RSV and strengthening global health defenses against respiratory viruses. However, *in vivo* studies are essential to validate the computational predictions and advance the vaccine candidate towards clinical application.

## Data availability statement

All data generated or analyzed during this study are included in this article.

## CRediT authorship contribution statement

**Truc Ly Nguyen:** Writing – review & editing, Writing – original draft, Visualization, Validation, Methodology, Investigation, Formal analysis, Data curation, Conceptualization. **Heebal Kim:** Writing – review & editing, Writing – original draft, Validation, Supervision, Resources, Investigation, Funding acquisition, Conceptualization.

## Declaration of competing interest

The authors declare that they have no known competing financial interests or personal relationships that could have appeared to influence the work reported in this paper.

## Acknowledgements

The authors are thankful to the Research Institute of Agriculture and Life Sciences, Seoul National University, and the BK21 FOUR Program of the Department of Agricultural Biotechnology, Seoul National University, Seoul, Republic of Korea, for supporting the research work. This research was supported by a fund (Project Code No. Z-1543082-2019-20-01) by Research of Animal and Plant Quarantine Agency, Republic of Korea.

## Appendix A. Supplementary data

Supplementary data to this article can be found online at <https://doi.org/10.1016/j.idm.2024.04.005>.

## References

Abraham, M. J., et al. (2015). Gromacs: High performance molecular simulations through multi-level parallelism from laptops to supercomputers. *SoftwareX*, 1–2, 19–25.

- Akhtar, N., et al. (2022). Immunoinformatics-Aided design of a peptide based multiepitope vaccine targeting glycoproteins and membrane proteins against monkeypox virus. *Viruses*, 14(11), 2374.
- Akhtar, N., et al. (2023). Secreted aspartyl proteinases targeted multi-epitope vaccine design for *Candida dubliniensis* using immunoinformatics. *Vaccines*, 11(2), 364.
- Andreatta, M., & Nielsen, M. (2016). Gapped sequence alignment using artificial neural networks: Application to the MHC class I system. *Bioinformatics*, 32(4), 511–517.
- Benkert, P., Biasini, M., & Schwede, T. (2010). Toward the estimation of the absolute quality of individual protein structure models. *Bioinformatics*, 27(3), 343–350.
- Bergeron, H. C., & Tripp, R. A. (2021). Immunopathology of RSV: An updated review. *Viruses*, 13(12), 2478.
- Borchers, A. T., et al. (2013). Respiratory syncytial virus—a comprehensive review. *Clinical Reviews in Allergy and Immunology*, 45(3), 331–379.
- Broor, S., Parveen, S., & Maheshwari, M. (2018). Respiratory syncytial virus infections in India: Epidemiology and need for vaccine. *Indian Journal of Medical Microbiology*, 36(4), 458–464.
- Bui, H.-H., et al. (2006). Predicting population coverage of T-cell epitope-based diagnostics and vaccines. *BMC Bioinformatics*, 7, 153, 153.
- Bui, H.-H., et al. (2007). Development of an epitope conservancy analysis tool to facilitate the design of epitope-based diagnostics and vaccines. *BMC Bioinformatics*, 8, 361, 361.
- Castiglione, F., et al. (2012). How the interval between prime and boost injection affects the immune response in a computational model of the immune system. *Computational and Mathematical Methods in Medicine*, 2012, 842329, 842329.
- Chawla, M., et al. (2023). Immunoinformatics-aided rational design of a multi-epitope vaccine targeting feline infectious peritonitis virus. *Frontiers in Veterinary Science*, 10.
- Ciarlito, C., et al. (2019). Respiratory syncytial virus A and B: Three bronchiolitis seasons in a third level hospital in Italy. *The Italian journal of pediatrics*, 45(1), 115, 115.
- Colosia, A., et al. (2023). Systematic literature review of the signs and symptoms of respiratory syncytial virus. *Influenza and other respiratory viruses*, 17(2), Article e13100.
- Conley, M. J., et al. (2022). Helical ordering of envelope-associated proteins and glycoproteins in respiratory syncytial virus. *The EMBO journal*, 41(3), Article e109728.
- Consortium, T. U. (2022). UniProt: The universal protein knowledgebase in 2023. *Nucleic Acids Research*, 51(D1), D523–D531.
- Cordeiro, P. A. S., et al. (2022). The role of IFN- $\gamma$  production during retroviral infections: An important cytokine involved in chronic inflammation and pathogenesis. *Revista do Instituto de Medicina Tropical de Sao Paulo*, 64, Article e64, e64.
- Cosentino, G., et al. (2022). Respiratory syncytial virus ribonucleoproteins hijack microtubule Rab11 dependent transport for intracellular trafficking. *PLoS Pathogens*, 18(7), Article e1010619.
- Dar, H. A., et al. (2022). Immunoinformatics-Aided analysis of RSV fusion and attachment glycoproteins to design a potent multi-epitope vaccine. *Vaccines*, 10(9), 1381.
- Dhanda, S. K., et al. (2013b). Prediction of IL4 inducing peptides. *Clinical and Developmental Immunology*, 2013, 263952, 263952.
- Dhanda, S. K., Vir, P., & Raghava, G. P. S. (2013). Designing of interferon-gamma inducing MHC class-II binders. *Biology Direct*, 8, 30, 30.
- Dimitrov, I., et al. (2013). AllergenFP: Allergenicity prediction by descriptor fingerprints. *Bioinformatics*, 30(6), 846–851.
- Dittmer, U., et al. (2001). Role of interleukin-4 (IL-4), IL-12, and gamma interferon in primary and vaccine-primed immune responses to Friend retrovirus infection. *Journal of Virology*, 75(2), 654–660.
- Doytchinova, I. A., & Flower, D. R. (2007). Vaxijen: A server for prediction of protective antigens, tumour antigens and subunit vaccines. *BMC Bioinformatics*, 8, 4, 4.
- Falsey, A. R., et al. (2005). Respiratory syncytial virus infection in elderly and high-risk adults. *New England Journal of Medicine*, 352(17), 1749–1759.
- Forstnerič, V., et al. (2017). The role of the C-terminal D0 domain of flagellin in activation of Toll like receptor 5. *PLoS Pathogens*, 13(8), Article e1006574.
- Garegnani, L., et al. (2021). Palivizumab for preventing severe respiratory syncytial virus (RSV) infection in children. *Cochrane Database of Systematic Reviews*, 11(11), Article CD013757. CD013757.
- Gasteiger, E., et al. (2005). Protein identification and analysis tools on the ExPASy server. In *The proteomics protocols handbook* (pp. 571–607). Humana Press.
- Chaffari-Nazari, H., et al. (2015). Improving multi-epitope long peptide vaccine potency by using a strategy that enhances CD4+ T help in BALB/c mice. *PLoS One*, 10(11), Article e0142563.
- Gupta, S., et al. (2013). In silico approach for predicting toxicity of peptides and proteins. *PLoS One*, 8(9), Article e73957.
- Gupta, S. K., et al. (2014). Flagellin a toll-like receptor 5 agonist as an adjuvant in chicken vaccines. *Clinical and Vaccine Immunology: CVI*, 21(3), 261–270.
- Harris, E. (2023). Cdc: RSV vaccine recommended for older people. *JAMA*, 330(5), 401.
- Jensen, K. K., et al. (2018). Improved methods for predicting peptide binding affinity to MHC class II molecules. *Immunology*, 154(3), 394–406.
- Jumper, J., et al. (2021). Highly accurate protein structure prediction with AlphaFold. *Nature*, 596(7873), 583–589.
- Kaushik, V., et al. (2022a). Immunoinformatics aided design and in-vivo validation of a cross-reactive peptide based multi-epitope vaccine targeting multiple serotypes of dengue virus. *Frontiers in Immunology*, 13, 865180, 865180.
- Kaushik, V., et al. (2022b). Immunoinformatics-Aided Design and in vivo Validation of a peptide-based multiepitope vaccine targeting canine circovirus. *ACS Pharmacology & Translational Science*, 5(8), 679–691.
- Kiss, G., et al. (2014). Structural analysis of respiratory syncytial virus reveals the position of M2-1 between the matrix protein and the ribonucleoprotein complex. *Journal of Virology*, 88(13), 7602–7617.
- Ko, J., et al. (2012). GalaxyWEB server for protein structure prediction and refinement. *Nucleic Acids Research*, 40(W1), W294–W297.
- Kozakov, D., et al. (2017). The ClusPro web server for protein–protein docking. *Nature Protocols*, 12(2), 255–278.
- Laham, F. R., et al. (2017). Clinical profiles of respiratory syncytial virus subtypes A and B among children hospitalized with bronchiolitis. *The Pediatric Infectious Disease Journal*, 36(8), 808–810.
- Larsen, J. E. P., Lund, O., & Nielsen, M. (2006). Improved method for predicting linear B-cell epitopes. *Immunome Research*, 2, 2, 2.
- Laskowski, R. A., et al. (1993). Procheck: A program to check the stereochemical quality of protein structures. *Journal of Applied Crystallography*, 26(2), 283–291.
- Laskowski, R. A., et al. (2018). PDBsum: Structural summaries of PDB entries. *Protein Science*, 27(1), 129–134.
- Li, Y., et al. (2015). Interaction between human BAP31 and respiratory syncytial virus small hydrophobic (SH) protein. *Virology*, 482, 105–110.
- Ma, Y., et al. (2020). Protective CD8+ T-cell response against Hantaan virus infection induced by immunization with designed linear multi-epitope peptides in HLA-A2.1/Kb transgenic mice. *Virology Journal*, 17(1).
- Marzec, J., et al. (2019). Toll-like receptor 4-mediated respiratory syncytial virus disease and lung transcriptomics in differentially susceptible inbred mouse strains. *Physiological Genomics*, 51(12), 630–643.
- Mejias, A., et al. (2019). Respiratory syncytial virus vaccines: Are we making progress? *The Pediatric Infectious Disease Journal*, 38(10), e266–e269.
- Messina, A., et al. (2022). New strategies for the prevention of respiratory syncytial virus (RSV). *Early Human Development*, 174, Article 105666.
- Mir, W. A. Y., et al. (2021). Successful treatment of respiratory syncytial virus infection in an immunocompromised patient with ribavirin. *Cureus*, 13(8), Article e16930.
- Moin, A. T., et al. (2023). A computational approach to design a polyvalent vaccine against human respiratory syncytial virus. *Scientific Reports*, 13(1), 9702, 9702.
- Monick, M. M., et al. (2003). Respiratory syncytial virus up-regulates TLR4 and sensitizes airway epithelial cells to endotoxin. *Journal of Biological Chemistry*, 278(52), 53035–53044.

- Morris, J. A., Blount, R. E., & Savage, R. E. (1956). Recovery of cytopathogenic agent from chimpanzees with goryza. *Experimental Biology and Medicine*, 92(3), 544–549.
- Nam, H. H., & Ison, M. G. (2019). Respiratory syncytial virus infection in adults. *BMJ*, 15021.
- Naqvi, S. T. Q., et al. (2021). Designing of potential polyvalent vaccine model for respiratory syncytial virus by system level immunoinformatics approaches. *BioMed Research International*, 2021, 9940010, 9940010.
- Nguyen, T. L., & Kim, H. (2024a). Discovering peptides and computational investigations of a multiepitope vaccine target *Mycobacterium tuberculosis*. *Synthetic and Systems Biotechnology*, 9(3), 391–405.
- Nguyen, T. L., & Kim, H. (2024b). Immunoinformatics and computational approaches driven designing a novel vaccine candidate against Powassan virus. *Scientific Reports*, 14(1), 5999.
- Obando, P., et al. (2018). Respiratory syncytial virus seasonality: A global overview. *The Journal of Infectious Diseases*, 217(9), 1356–1364.
- Rapin, N., Lund, O., & Castiglione, F. (2011). Immune system simulation online. *Bioinformatics*, 27(14), 2013–2014.
- Robinson, C. L., et al. (2017). Advisory committee on immunization practices recommended immunization schedule for children and adolescents aged 18 Years or younger - United States, 2017. *MMWR. Morbidity and mortality weekly report*, 66(5), 134–135.
- Ruckwardt, T. J. (2023). The road to approved vaccines for respiratory syncytial virus. *NPJ vaccines*, 8(1), 138, 138.
- Ruckwardt, T. J., Morabito, K. M., & Graham, B. S. (2019). Immunological lessons from respiratory syncytial virus vaccine development. *Immunity*, 51(3), 429–442.
- Shanmugam, A., et al. (2012). Synthetic Toll like receptor-4 (TLR-4) agonist peptides as a novel class of adjuvants. *PLoS One*, 7(2), Article e30839.
- Shen, Z., et al. (2022). Rapid typing diagnosis and clinical analysis of subtypes A and B of human respiratory syncytial virus in children. *Virology Journal*, 19(1), 15, 15.
- Tahir Ul, M., et al. (2020). Multiepitope-based subunit vaccine design and evaluation against respiratory syncytial virus using reverse vaccinology approach. *Vaccines*, 8(2), 288.
- Topalidou, X., Kalergis, A. M., & Papazisis, G. (2023). Respiratory syncytial virus vaccines: A review of the candidates and the approved vaccines. *Pathogens*, 12(10), 1259.
- Vandini, S., Biagi, C., & Lanari, M. (2017). Respiratory syncytial virus: The influence of serotype and genotype variability on clinical course of infection. *International Journal of Molecular Sciences*, 18(8), 1717.
- Vangone, A., et al. (2011). Cocomaps: A web application to analyze and visualize contacts at the interface of biomolecular complexes. *Bioinformatics*, 27(20), 2915–2916.
- Wiederstein, M., & Sippl, M. J. (2007). ProSA-web: Interactive web service for the recognition of errors in three-dimensional structures of proteins. *Nucleic Acids Research*, 35(Web Server issue), W407–W410.